

# DFT study of the molecular structure of 3,4-dihydropyrimidin-2(1*H*)-ones

Hamid Reza Memarian · Hassan Sabzyan · Asadollah Farhadi

Received: 12 April 2010 / Accepted: 11 August 2010 / Published online: 9 September 2010  
© Springer-Verlag 2010

**Abstract** Density functional theory at B3LYP/6-31++G(d,p) level was applied to study structural, electronic, and bonding characteristics of some 3,4-dihydropyrimidin-2(1*H*)-ones substituted at C4 position (DHPMs) of pharmaceutical interest. Results of this study show that in these DHPMs the six-membered ring adopts a *pseudo-boat* conformation with a *pseudo-axial* orientation of the C4 substituent, and the heights of the C4 and N4 atoms from the boat plane depend on the type and position of the substituent on the aryl ring. Thermochemical analysis of these DHPMs and their corresponding oxidation products shows that the enthalpy of the oxidation reaction depends on the nature of the substituent at the C4 position, falling in a range of 25 kJ/mol for all compounds.

**Keywords** Dihydropyrimidinones · B3LYP/6-31++G(d,p) · Oxidation rate · Conformational analysis

## Introduction

Alkaloid systems, including 3,4-dihydropyrimidin-2(1*H*)-ones (DHPMs), are heterocyclic compounds of great pharmacological importance [1–3]. DHPMs have been used as calcium channel modulators [4], antihypertensive agents [5], anticancer agents [6], antibacterial agents, and

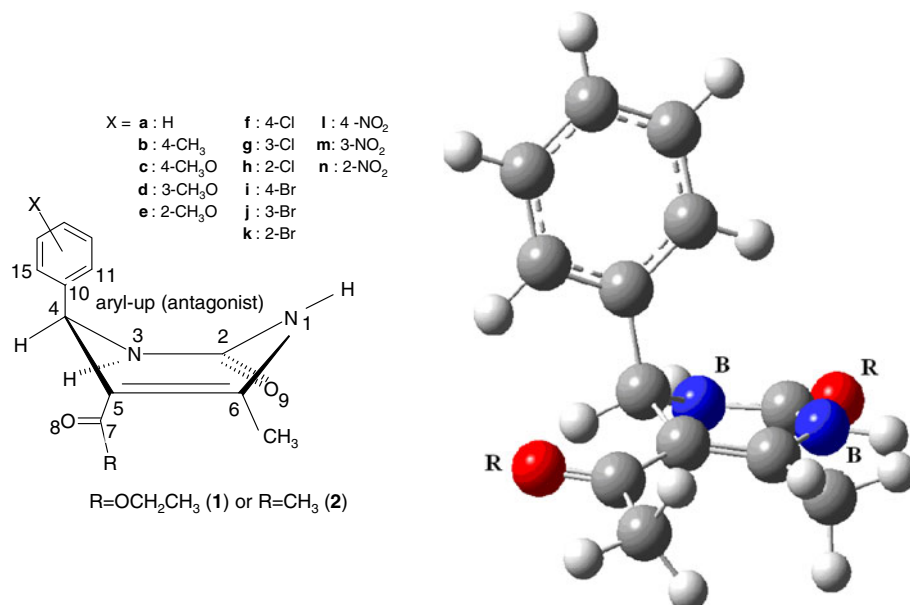
antistaphylococcal antibiotics [7]. Many experimental studies have been carried out on the simpler relatives of DHPMs, i.e., 1,4-dihydropyridines (DHPs) [8–14]. Structure–function relationships of DHPMs have also been studied [15–18]. However, there are still debates on the exact stereochemical/conformational requirements for their pharmacological activities [19–21]. Triggle and Padmanabhan [22] reported a detailed structure–activity profile for a series of DHPMs as calcium channel modulators, leading to a new general binding-site model. Furthermore, it is found that the activation of DHPMs as calcium channel modulators depends on the absolute configuration at the stereogenic center (C4 position; Fig. 1). In this context, alternation of the orientation of the 4-substituent group (*R/S* enantiomers) acts as “molecular switching” between antagonist and agonist activities [23]. To develop quantitative structure–activity models or to perform molecular docking simulations on the drug–receptor interaction, it is essential to have reliable, well-examined methods at hand to study the geometry and conformational hypersurface of molecules with biological properties of interest. In the case of the DHP series of molecules, the effect of conformational changes on the calcium channel modulatory activity are well documented by many pharmacological studies [19, 20], and numerous computational and experimental studies investigating the conformational hypersurface of these systems have been reported [24–27].

Structural studies of several DHPMs have shown that (a) changing the configuration of the C4 position affects their biological activities, and (b) the configuration of the substituent at C5 position plays a major role in the pharmacological activity of these compounds. For the DHPM series of compounds, application of circular dichroism (CD) and X-ray crystal data of individual pure enantiomers, referenced to samples of known absolute configuration, have proven

H. R. Memarian (✉) · H. Sabzyan (✉) · A. Farhadi  
Department of Chemistry, Faculty of Science,  
University of Isfahan, 81746-73441 Isfahan, Iran  
e-mail: memarian@sci.ui.ac.ir

H. Sabzyan  
e-mail: sabzyan@sci.ui.ac.ir

**Fig. 1** General structure of the ethyl ester (**1**) and acetyl (**2**) derivatives of dihydropyrimidinones (DHPMs, denoted in the text as EDHMPs and ADHMPs, respectively) with aryl-up conformation, and the numbering scheme used in this work. An example of the optimized structures of DHPMs is given on the right. The red (R) and blue balls (B) represent the oxygen and nitrogen atoms, respectively



useful for determination of the absolute configuration in various biologically active DHPM derivatives. In these studies, it is found that only molecules with *R* configuration act as calcium channel modulators [23, 28–31]. Results of computations at ab initio (HF and B3LYP) and semi-empirical (AM1 and PM3) levels of theory carried out on the conformational analysis of some DHPMs are in agreement with the X-ray crystallographic data [3, 32, 33]. These results indicate the importance of computational studies both as complements to experimental work and as replacement tools for structure–activity studies on compounds of pharmacological importance.

Due to the importance of the configuration of the aryl group at the C4 position of the heterocyclic ring for the biological and pharmacological activities of DHPMs, in the present work we used B3LYP/6-31++G(d,p) computations to study structural, bonding, and spectroscopic characteristics of a series of DHPMs. General structures of the DHPMs with aryl-up (antagonist) conformation studied in this work are shown in Fig. 1. These characteristics include bond lengths and angles, charge density, hybridization of some relevant atoms, and deviation of the C4 and N1 atoms from the boat ring base plane. To obtain enthalpies for the gas-phase oxidation reactions of DHPMs, it was also necessary to carry out vibrational analysis and calculate the heats of formation for the corresponding oxidation products, the pyrimidinones. The rate of oxidation of DHPMs by potassium peroxydisulfate in a mixture of acetonitrile and water, obtained under different reaction conditions in independent experimental works reported elsewhere [34–36], are correlated with the results of this computational study. It should be noted here that the optimum structures of some DHPMs have already

been studied using computational techniques [3, 32, 37]. However, the characteristics studied in this work have not been studied so far.

## Results and discussion

The general structure of ethyl 4-aryl-1,2,3,4-tetrahydro-6-methyl-2-oxypyrimidine-5-carboxylates (EDHMPs) and 5-acetyl-4-aryl-1,2,3,4-tetrahydro-6-methyl-2-oxypyrimidines (ADHMPs) are shown in Fig. 1, where the numbering scheme used to describe these structures is also introduced. Analysis of the optimized structures of EDHMPs and ADHMPs shows that the six-membered ring adopts a *boat* conformation, flattened at N1 toward an envelope conformation, with a *pseudo-axial* orientation of the C4 substituent. Thus, in all derivatives the C4 substituent adopts an *up* orientation with respect to the heterocyclic ring boat plane. This orientation corresponds to the antagonist activity of these compounds. The same structural trends had already been observed for the 1,4-dihydropyridines (DHPs) [21]. Therefore, similar activities are expected for corresponding DHPMs and DHPs.

In Tables 1 and 2, the optimized lengths of the C7=O8, C5=C6, C2=O9, N1–H, N3–H, and C4–H bonds that play a role in the activities of DHPMs are listed. Furthermore, the optimum values of the C6–C5–C7–O8, C11–C10–C4–N3, and C11–C10–C4–C5 dihedral angles, denoted by  $\alpha$ ,  $\beta$ , and  $\gamma$ , respectively, and reported in Tables 1 and 2, reflect the orientations of the carbonyl group and the aryl ring on the C5 and C4 positions with respect to the heterocyclic ring. The optimum values of the dihedral angle  $\beta$  show that the aryl and DHPM rings are not perpendicular to each other.

**Table 1** Selected B3LYP/6-31++G(d,p) optimized geometrical parameters obtained for EDHPMs (bond lengths and angles are given in Å and degrees, respectively)

Comp.	C7=O8 (Å)	C5=C6 (Å)	C2=O9 (Å)	N1–H (Å)	N3–H (Å)	C4–H (Å)	$\alpha$ (°)	$-\beta$ (°)	$\gamma$ (°)	$\Delta$ (°)
<b>1a</b>	1.2258	1.3657	1.2267	1.0102	1.0115	1.0928	174.0	42.7	81.5	38.8
<b>1b</b>	1.2256	1.3656	1.2267	1.0102	1.0115	1.0928	173.4	45.7	78.5	32.8
<b>1c</b>	1.2256	1.3647	1.2270	1.0101	1.0115	1.0930	174.7	50.4	73.9	23.5
<b>1d</b>	1.2244	1.3646	1.2268	1.0102	1.0115	1.0926	173.2	40.8	83.3	42.5
<b>1e</b>	1.2214	1.3650	1.2221	1.0094	1.0101	1.0921	178.8	113.0	11.4	-101.6
<b>1f</b>	1.2251	1.3650	1.2262	1.0105	1.0115	1.0926	175.3	36.3	87.7	51.4
<b>1g</b>	1.2252	1.3653	1.2257	1.0103	1.0104	1.0927	174.8	42.0	82.3	40.3
<b>1h</b>	1.2250	1.3663	1.2260	1.0096	1.0110	1.0949	168.2	62.8	64.4	1.6
<b>1i</b>	1.2256	1.3652	1.2262	1.0105	1.0115	1.0926	174.3	31.0	92.8	61.8
<b>1j</b>	1.2254	1.3655	1.2257	1.0105	1.0114	1.0925	175.3	38.3	85.8	47.5
<b>1k</b>	1.2250	1.3666	1.2259	1.0096	1.0110	1.0957	168.2	64.5	62.8	-1.7
<b>1l</b>	1.2248	1.3686	1.2247	1.0104	1.0112	1.0949	177.4	33.0	91.0	58.0
<b>1m</b>	1.2254	1.3664	1.2245	1.0105	1.0114	1.0931	178.4	58.4	65.9	7.5
<b>1n</b>	1.2261	1.3684	1.2248	1.0098	1.0108	1.0959	172.5	84.4	43.9	-40.5

See Fig. 1 for numbering scheme

**Table 2** Selected B3LYP/6-31++G(d,p) optimized geometrical parameters obtained for ADHPMs (bond lengths and angles are given in Å and degrees, respectively)

Comp.	C7=O8 (Å)	C5=C6 (Å)	C2=O9 (Å)	N1–H (Å)	N3–H (Å)	C4–H (Å)	$\alpha$ (°)	$-\beta$ (°)	$\gamma$ (°)	$\Delta$ (°)
<b>2a</b>	1.2269	1.3638	1.2188	1.0091	1.0099	1.0896	175.0	36.1	88.5	52.4
<b>2b</b>	1.2340	1.3678	1.2268	1.0105	1.0115	1.0917	174.7	39.0	85.5	46.5
<b>2c</b>	1.2341	1.3679	1.2268	1.0105	1.0116	1.0917	175.3	43.8	82.8	40.6
<b>2d</b>	1.2343	1.3684	1.2263	1.0106	1.0115	1.0917	175.0	29.9	94.6	64.7
<b>2e</b>	1.2342	1.3689	1.2278	1.0095	1.0115	1.0928	169.8	58.6	68.5	9.9
<b>2f</b>	1.2345	1.3681	1.2260	1.0108	1.0115	1.0917	177.7	30.3	94.0	63.7
<b>2g</b>	1.2344	1.3685	1.2255	1.0108	1.0114	1.0917	176.0	34.1	90.5	56.4
<b>2h</b>	1.2342	1.3691	1.2259	1.0097	1.0111	1.0939	167.2	63.3	64.6	1.3
<b>2i</b>	1.2346	1.3682	1.2259	1.0108	1.0115	1.0917	177.5	28.2	96.0	67.8
<b>2j</b>	1.2345	1.3686	1.2254	1.0108	1.0114	1.0916	177.2	36.6	88.0	51.4
<b>2k</b>	1.2339	1.3685	1.2259	1.0096	1.0111	1.0948	163.7	65.1	62.7	-2.4
<b>2l</b>	1.2345	1.3686	1.2248	1.0110	1.0115	1.0919	178.0	27.7	96.8	69.1
<b>2m</b>	1.2345	1.3688	1.2243	1.0108	1.0114	1.0920	179.3	52.3	72.5	20.2
<b>2n</b>	1.2352	1.3714	1.2248	1.0100	1.0109	1.0950	172.2	85.0	43.8	-41.2

See Fig. 1 for numbering scheme

Deviation of the dihedral angle  $\beta$  from 90° (denoted by  $\Delta$ ) is calculated using Eq. 1 as follows, and the results are reported in Tables 1 and 2. This definition of the dihedral angle deviation denotes the deviation of the aryl ring towards the N3 and C5 atoms by positive and negative values of  $\Delta$ .

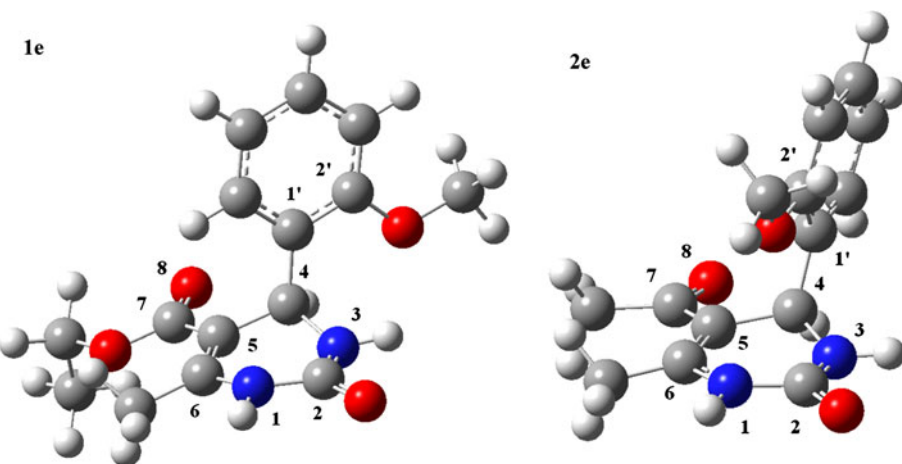
$$\Delta = \gamma + \beta. \quad (1)$$

Analysis of the  $\alpha$  dihedral angles shows that in all cases the carbonyl group deviates from the coplanar conformation with respect to the DHPM boat plane. However, the

conformations of the carboethoxy and the acetyl groups can be considered approximately as *s-trans* with respect to their adjacent C5=C6 bonds of the DHPM ring. The observation of the exceptionally high deviation  $\Delta$  for **1e** (-110.6°) compared with **2e** (+9.9°) is possibly due to the orientation of the 2-methoxy group outside the heterocyclic ring in **1e** compared with the inside orientation of this group in **2e** (Fig. 2).

The results reported in Tables 1 and 2 show that the C7=O8 bond length is correlated with the dihedral angle  $\alpha$ . Other parameters, such as the deviation of the N1 atom

**Fig. 2** Optimized structures of **1e** and **2e** obtained at B3LYP/6-31++G(d,p) level of theory



from the boat plane, can also affect this bond length. The optimized structural parameters show that partial conjugation of the C5=C6 and C7=O8 groups depends on the  $\alpha$  dihedral angle, since approach of the C7=O8 group towards the coplanar conformation results in an increase in the C7=O8 and C5=C6 bond lengths, and a decrease in the C5-C7 bond length. For example, the  $\alpha$  dihedral angles of **1a** and **1k**, 168.2° and 174.0°, correspond to C7=O8, C5=C6, and C5-C7 bond lengths of 1.2250 and 1.2258 Å, 1.3657 and 1.3666 Å, and 1.4682 and 1.4676 Å, respectively. Comparative analysis shows that the C7=O8 bond length is longer in the ADHPMs series than the corresponding one in the EDHPMs series. It should be noted that the balance between the resonance and the inductive effects of the ethoxy group as compared with the inductive effect of the methyl group determines the conformational structure of the EDHPMs compared with that of the ADHPMs. For example, the C7=O8 bond length in **1e** and **2e** is 1.2214 and 1.2342 Å, corresponding to the  $\alpha$  dihedral angles of 177.8° and 169.8°, which is opposite to the trend reported above.

Review of the data reported in Tables 1 and 2 shows that the C2=O9 bond lengths in the corresponding ADHPMs and EDHPMs are very close, while they are dependent on the type of the substituent at the C4 position.

In general, the N1-H bond length is very close to the N3-H bond length in all ADHPMs and EDHPMs, and both vary slightly with the substituent at the C4 position.

The C4-H bond length is generally larger in the EDHPM series and depends strongly on the substituents at the C4 and C5 positions. The optimized conformation of the aryl ring, described by the dihedral angle  $\beta$ , is affected by the substituents on the aryl ring, which act via interaction with the substituents or the lone pairs on the N3 atom. The relation of this structural parameter with the deviation of the C4 and N1 atoms from the boat plane is investigated in the next section.

#### Deviation of the N1 and C4 atoms from the boat plane (C2-N3-C5-C6)

Since deviations of the N1 and C4 atoms of the heterocyclic ring of the DHPMs (referenced to the plane containing C2, N3, C5, and C6 atoms) from the boat plane affect the rate of their oxidation, calculations and analyses of these deviations are described in this section. These calculations are based on the geometries and trigonometrics given in Figs. 3 and 4. For these calculations, we obtained the  $\theta_1$ ,  $\varphi_1$ ,  $\alpha_1$ , and  $\alpha_2$  angles and the C2-C6 distance from the optimized structures of DHPMs using the trigonometric relations (2–14). The same algorithm is used for the calculation of the deviation of the C4 atom from the same boat plane ( $h_C$ ); the only difference is that the geometry is based on the N3-C4-C5 triangle (Fig. 3). The calculated values of the deviation of the N1 ( $h_N$ ) and C4 ( $h_C$ ) atoms of the EDHPMs and ADHPMs are reported in Table 3. The data reported in this table show that the deviations of the N1 atom from the boat plane in ADHPMs are larger than that in EDHPMs, while the deviations of the C4 atom in EDHPMs and ADHPMs are nearly equal. As mentioned

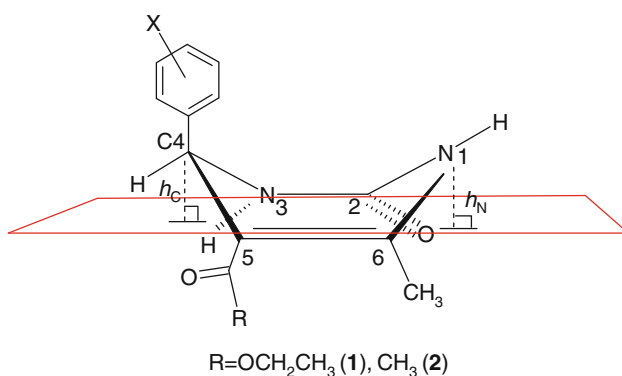


**Fig. 3** General geometry defining the deviation of the N1 and C4 atoms from the boat plane (C2-N3-C5-C6) in the DHPMs

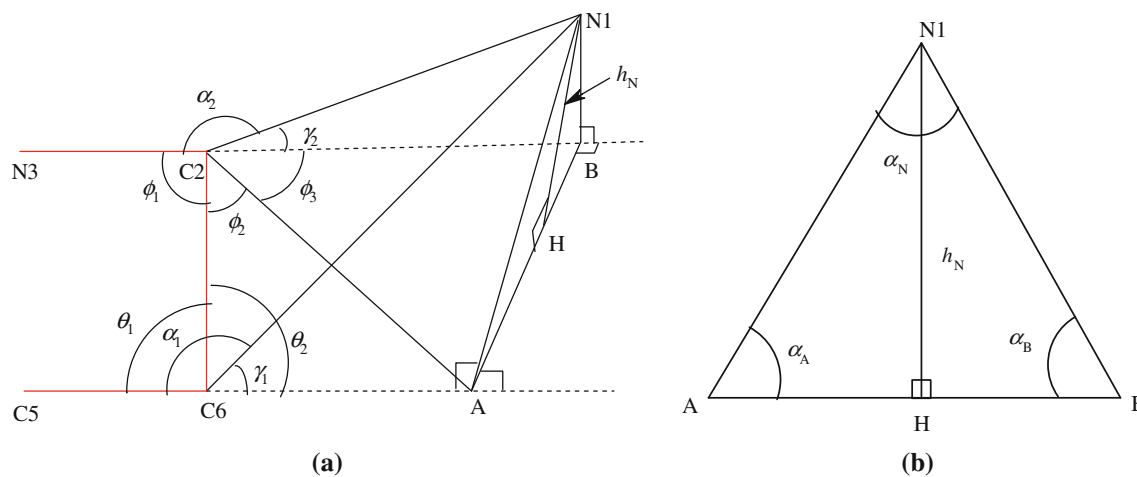


**Fig. 4** **a** The trigonometric frame used for the calculation of the deviation of the N1 atom (the height  $h_N$ ) from the C2–N3–C5–C6 plane (Fig. 3), and **b** a closer view of the triangle defining the height of the N1 atom ( $h_N$ ) from the C2–N3–C5–C6 plane as shown in **(a)**

**Table 3** Values of the deviations  $h_N$  (N1) and  $h_C$  (C4) ( $\text{\AA}$ ) from the boat plane (C2–N3–C5–C6) based on the geometries given in Figs. 3 and 4 calculated by using relations (2–12) for DHPMs

Compound	EDHPMs		ADHPMs	
	$h_N$ (N1) ( $\text{\AA}$ )	$h_C$ (C4) ( $\text{\AA}$ )	$h_N$ (N1) ( $\text{\AA}$ )	$h_C$ (C4) ( $\text{\AA}$ )
<b>a</b>	0.1276	1.0829	0.3654	1.0930
<b>b</b>	0.1231	1.0825	0.1444	1.0626
<b>c</b>	0.1119	1.0858	0.2908	1.0920
<b>d</b>	0.1296	1.0845	0.1561	1.0977
<b>e</b>	0.1407	1.1222	0.2115	1.0774
<b>f</b>	0.1336	1.0865	0.1626	1.0991
<b>g</b>	0.2080	1.0811	0.1528	1.0921
<b>h</b>	0.0476	1.0824	0.1220	1.0534
<b>i</b>	0.1427	1.0886	0.1618	1.1000
<b>j</b>	0.1438	1.0878	0.2024	1.0960
<b>k</b>	0.1230	1.0465	0.0237	1.0474
<b>l</b>	0.1431	1.0324	0.1656	1.0985
<b>m</b>	0.1147	1.0755	0.1193	1.1212
<b>n</b>	0.0322	1.0517	0.0216	1.0534

earlier, the C5=C6 bond length is correlated with the deviation of the N1 atom. Analysis of the data reported in Table 3 shows also that a decrease in the height of the N1 atom ( $h_N$ ) from the boat plane increases the possibility of conjugation of the N1 lone-pair electrons with the C5=C6 group, which results in an increase in the C5=C6 bond lengths and a decrease in the C6–N1 bond lengths. For example, in **1f** and **1h**, the C5=C6 and C6–N1 bond lengths are 1.3650 and 1.3663  $\text{\AA}$ , and 1.3862 and 1.3795  $\text{\AA}$ , corresponding, respectively, to 0.1336 and 0.0476  $\text{\AA}$  heights of the N1 atom. An opposite trend is observed for the **1c** and **1e** pair.

$$\gamma_1 = 180 - \alpha_1 \quad (2)$$

$$\gamma_2 = 180 - \alpha_2 \quad (3)$$

$$\theta_2 = 180 - \theta_1 \quad (4)$$

$$C6A = C6N \cos \gamma_1 \quad (5)$$

$$C2B = C2N \cos \gamma_2 \quad (6)$$

$$NA = C6N \sin \gamma_1 \quad (7)$$

$$NB = C2N \sin \gamma_2 \quad (8)$$

$$C2A = (C6A^2 + C2C6^2 - 2C6A \times C2C6 \times \cos(\theta_2))^{1/2} \quad (9)$$

In triangle AC2C6 :

$$\cos(\varphi_2) = \frac{(C2C6)^2 + (C2A)^2 - (C6A)^2}{2 C6C2 \times C2A} \quad (10)$$

$$\varphi_3 = 180 - (\varphi_1 + \varphi_2) \quad (11)$$

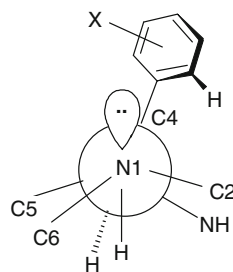
In triangle ABC2 :

$$AB = (C2A^2 + C2B^2 - 2C2A \times C2B \times \cos(\varphi_3))^{1/2} \quad (12)$$

$$\text{In triangle ABN1 : } \cos(\alpha_B) = \frac{NB^2 + AB^2 - NA^2}{2NB \times AB} \quad (13)$$

$$\text{In triangle HBN1 : } NH = NB \times \sin(\alpha_B) \quad (14)$$

To investigate the effect of the substituent on the aryl ring at the C4 position of the DHPM heterocyclic ring on the deviation of this ring from planar conformation, we used the Newman-like model below in which the N1 and C4 atoms are superimposed as shown in Scheme 1. Based on this model and considering the  $h_C$  and  $h_N$  deviations reported in Table 3, and dihedral angle deviations  $\Delta$  (introduced in Eq. 1 and reported in Tables 1 and 2), we

**Scheme 1**

observe that distancing  $\Delta$  from zero influences the interaction of the *ortho* hydrogen or the *ortho* substituents on the aryl ring with the atoms of the heterocyclic ring, and thus influences the height of the N1 atom from the boat plane ( $h_N$ ). In terms of natural bond orbital (NBO) terminology, the balance between donor–acceptor interactions of different bonds/atoms of the aryl ring and those of the heterocyclic ring plus induction and resonance effects of the substitution on the aryl ring determines the values of  $\Delta$ . No pure trend could be extracted for individual contributions. For example, the height of the N1 atom in **1a** and **2b** with repulsive interaction is 0.1276 and 0.1231 Å, corresponding to  $\Delta$  dihedral angles 38.8° and 32.8°; in contrast, the height  $h_N$  in **1i** and **1j** with attractive interactions is 0.1427 and 0.1438 Å, corresponding to  $\Delta$  values of 61.8° and 47.5°.

Analysis of the data reported in the Table 4 shows that deviation of the C4 atom from the boat plane also depends on the type and position of the substituent on the aryl ring. For example, in the **1c** and **1e** isomers with the same

substituent (methoxy) on the 4- and 2-positions of the aryl ring, this deviation is smaller for the former isomer (1.0858 versus 1.1222 Å). As described for the deviation of the N1 atom, the extent of the deviation of the C4 atom depends on the type of the interaction of the *ortho* hydrogen or the substituents on the aryl ring with the atoms of the heterocyclic ring. Figure 5 shows the correlation between the deviation of the C4 and N1 atoms from the boat ring and the type and position of the substituent on the aryl ring at the C4 position of the DHPM ring.

#### Natural bond orbital analysis

The NBO electric charges calculated for selected atoms including N1, N3, N1–H, N3–H, and C4–H, which are important in the oxidation reactivity of the DHPMs, are listed in Table 4. In this table, the calculated electric dipole moments ( $\mu$ ) of DHPMs are also reported. Analysis of the data shows that the charge densities on these atoms depend on the type and position of the substituent on the aryl ring showing the inductive and resonance effects, and through-space interactions of the substituent on the aryl ring (located at the C4 position) with these atoms. Since the charge of the N1, N3, N1–H, N3–H, and C4–H atoms in the EDHPM and ADHPM series are more or less very close (compound **1l** is an exception), it can be concluded that the through-bond inductive effects of the substitution on the aryl ring do not contribute to the structural characteristics of the DHPM heterocyclic ring.

**Table 4** Natural bond orbital (NBO) analysis of the atomic charges and electric dipole moments calculated for DHPMs using B3LYP/6-31++G(d,p) method

Comp.	$\mu$ (D)	EDHPMs					ADHPMs					
		N1–H	N3–H	C4–H	N1	N3	$\mu$ (D)	N1–H	N3–H	C4–H	N1	N3
<b>a</b>	3.958	+0.446	+0.444	+0.274	-0.654	-0.663	3.854	+0.407	+0.407	+0.239	-0.631	-0.635
<b>b</b>	3.892	+0.446	+0.443	+0.274	-0.655	-0.665	3.832	+0.445	+0.372	+0.280	-0.656	-0.663
<b>c</b>	4.177	+0.446	+0.443	+0.272	-0.656	-0.662	3.761	+0.445	+0.444	+0.278	-0.656	-0.660
<b>d</b>	4.109	+0.369	+0.444	+0.293	-0.652	-0.671	4.060	+0.445	+0.445	+0.282	-0.654	-0.661
<b>e</b>	2.146	+0.400	+0.444	+0.293	-0.652	-0.671	4.339	+0.442	+0.441	+0.274	-0.644	-0.663
<b>f</b>	4.676	+0.447	+0.445	+0.277	-0.654	-0.666	4.643	+0.446	+0.445	+0.283	-0.655	-0.664
<b>g</b>	4.782	+0.447	+0.445	+0.276	-0.654	-0.664	4.366	+0.447	+0.446	+0.283	-0.655	-0.665
<b>h</b>	3.889	+0.447	+0.444	+0.265	-0.646	-0.665	3.174	+0.446	+0.444	+0.270	-0.646	-0.661
<b>i</b>	4.667	+0.447	+0.445	+0.278	-0.653	-0.664	4.634	+0.446	+0.446	+0.283	-0.655	-0.664
<b>j</b>	4.840	+0.447	+0.445	+0.278	-0.654	-0.663	4.364	+0.447	+0.446	+0.283	-0.655	-0.665
<b>k</b>	3.854	+0.447	+0.444	+0.263	-0.647	-0.664	3.067	+0.446	+0.445	+0.267	-0.647	-0.662
<b>l</b>	7.163	+0.280	+0.280	+0.140	-0.605	-0.541	7.218	+0.448	+0.447	+0.286	-0.665	-0.666
<b>m</b>	6.300	+0.449	+0.444	+0.273	-0.654	-0.665	5.559	+0.449	+0.446	+0.278	-0.665	-0.666
<b>n</b>	3.951	+0.449	+0.442	+0.263	-0.637	-0.663	2.394	+0.449	+0.442	+0.268	-0.636	-0.660

See Fig. 1 for numbering scheme

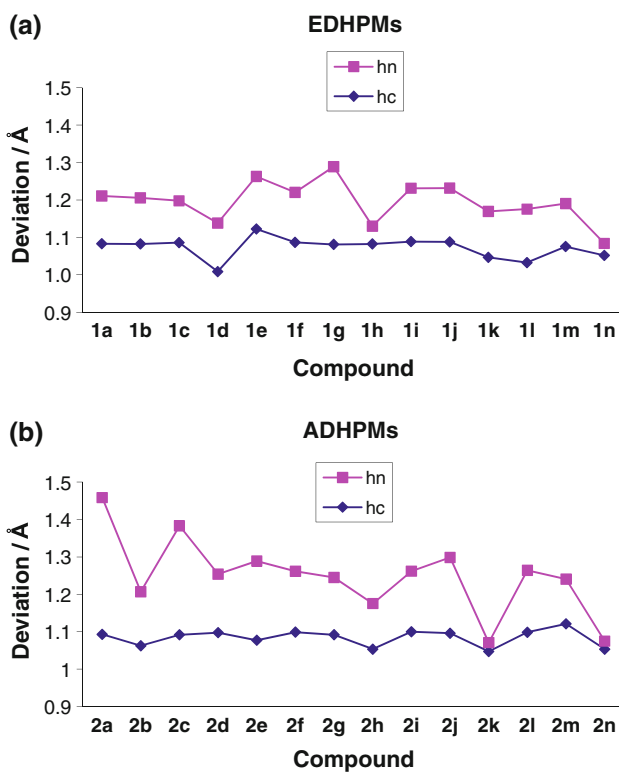


**Fig. 5** Correlation between deviations of the N1 and C4 atoms from the boat plane and the type and position of the substituent on the aryl ring for **a** EDHPMs and **b** ADHPMs

A review of the data reported in Table 4 shows also that the charge density on the N1 atom is slightly smaller than that on the N3 atom, because its electrons can participate in a resonance with the C2=O9 and C5=C6 double bonds, while the electrons of N3 can only resonate with the C2=O9 bond. Furthermore, direct through-space interactions between atoms or groups of atoms, and the deviation of the N1 atom from the boat plane, may also affect the charge density on these atoms. This clearly shows that any nucleophilic attack at the N1–H and N3–H centers is affected by the substituent at the C4 position [34–36].

The dipole moment ( $\mu$ ) data reported in Table 4 fall in the range of 2.146–7.218 D, showing that all of the DHPM compounds are polar, but their per-volume polarity is low. Therefore, it can be predicted that solubilities of DHPMs in water are low, which is compatible with what is observed experimentally [34–36]. The overall dipole moment of a DHPM compound is a result of interplay between the chemical bonding and structure of both the aryl and heterocyclic rings. Due to the complexity of this interplay, analysis of the dipole moment data does not show any correlation between the dipole moments of the EDHPMs and ADHPMs series.

Atomic hybridizations were calculated within NBO theory for the B3LYP/6-31++G(d,p) optimized structures

of DHPMs. In general, overall hybridization of the N1, N3, and C4 atoms and the partial hybridization of the C4 atom in the C4–C10 bond in the DHPM series vary slightly with the substituent on the aryl ring at the C4 position, and fall in the range of  $sp^{2.55}$ – $sp^{2.66}$ ,  $sp^{2.97}$ – $sp^{3.02}$ ,  $sp^{1.81}$ – $sp^{1.85}$ , and  $sp^{1.88}$ – $sp^{1.89}$ . A detailed analysis showed that the hybridization data cannot be used to justify the structural features of DHPMs.

#### Vibration analysis

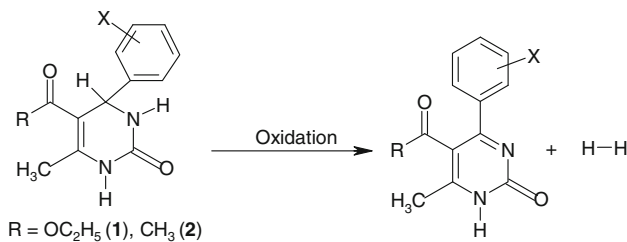
Vibration analysis was carried out on the optimized geometries of the DHPMs at B3LYP/6-31++G(d,p) level of theory using a scale factor of 0.8929. The harmonic frequencies calculated for DHPMs along with their IR intensities (given in parentheses) are reported in Table 5. As expected, the calculated vibrational frequencies show dependence on the type and position of the substituent. In all DHPMs the frequency of the N1–H bond stretching mode is larger than that of the N3–H bond. This can be attributed to the tighter conjugation of the N1 atom with the C5=C6 bond and the C7=O8 group, as compared with that of the N3 atom, which results in a stronger N1–H bond. Furthermore, smaller frequencies of the stretching mode of the C7=O8 group, as compared with those of the C2=O9 group, can also be attributed to the fact that the C7=O8 bond is conjugated with the C5=C6 group and N1 atom, while the C2=O9 bond is conjugated only to the N3 atom.

#### Thermochemical analysis

Standard formation enthalpies ( $\Delta H_f^\circ$ ) and the enthalpies of the oxidation reaction ( $\Delta H_{ox}^\circ$ ) of DHPMs were calculated based on the reaction given in Scheme 2 using the B3LYP/6-31++G(d,p) enthalpies calculated for H<sub>2</sub>, EDHPMs, ADHPMs, and their corresponding oxidation products, i.e., esteric and ketonic pyrimidinones (EPMs and APMs). In these calculations, the enthalpy change due to the reduction of the oxidant (which is identical for all reactions) is not considered for brevity. Furthermore, all calculated oxidation enthalpies are referenced to that of the corresponding 4-phenyl derivatives (compound a). Results of these calculations and the corresponding formation enthalpies are reported in Table 6. This thermochemical analysis of the oxidation reactions can only be used on a comparative basis. The obtained data show that the oxidation enthalpies of the EDHPMs and ADHPMs fall within the range of (−15.4, +10.9) and (−15.1, +4.2) kJ/mol as referenced to those of the compound a. Although these variations fall outside of the typical error bars of the B3LYP calculations, they are not large enough to be used for justification of the differences observed for the comparative rates of oxidation. This means, in other words, that any observed differences

**Table 5** Calculated harmonic frequencies ( $\text{cm}^{-1}$ ) (IR intensities) obtained for the B3LYP/6-31++G(d,p) optimized structures of DHPMs

	C4–H ( $\text{\AA}$ )	N1–H ( $\text{\AA}$ )	N3–H ( $\text{\AA}$ )	C2=O9 ( $\text{\AA}$ )	C5=C6 ( $\text{\AA}$ )	C7=O8 ( $\text{\AA}$ )
EDHPMs						
<b>a</b>	3,090.5 (5.5)	3,644.2 (75.9)	3,628.9 (44.2)	1,788.1 (717.8)	1,669.1 (191.6)	1,728.0 (396.0)
<b>b</b>	3,091.8 (5.9)	3,644.7 (76.1)	3,628.6 (42.8)	1,787.4 (725.6)	1,670.2 (190.0)	1,728.9 (398.3)
<b>c</b>	3,088.6 (6.4)	3,646.0 (77.6)	3,627.9 (41.6)	1,787.2 (735.5)	1,670.6 (173.6)	1,729.2 (399.6)
<b>d</b>	3,090.7 (6.3)	3,646.7 (78.5)	3,626.9 (40.0)	1,788.0 (738.1)	1,672.2 (203.1)	1,733.8 (398.2)
<b>e</b>	3,109.1 (0.9)	3,642.9 (72.4)	3,627.6 (57.2)	1,787.1 (717.8)	1,668.2 (199.7)	1,733.9 (431.3)
<b>f</b>	3,095.0 (4.4)	3,642.5 (77.3)	3,628.9 (45.8)	1,789.5 (711.9)	1,668.3 (192.4)	1,725.3 (400.7)
<b>g</b>	3,093.4 (4.9)	3,642.2 (76.7)	3,630.1 (46.8)	1,791.1 (700.9)	1,668.2 (189.5)	1,726.5 (387.3)
<b>h</b>	3,055.8 (10.9)	3,653.1 (84.0)	3,635.1 (41.9)	1,791.0 (757.2)	1,670.1 (222.2)	1,727.3 (388.0)
<b>i</b>	3,096.4 (3.7)	3,643.1 (77.1)	3,629.7 (46.2)	1,789.8 (704.2)	1,667.9 (189.4)	1,724.4 (404.3)
<b>j</b>	3,095.0 (4.5)	3,642.9 (75.9)	3,630.3 (46.9)	1,791.4 (682.8)	1,668.0 (184.8)	1,725.9 (385.0)
<b>k</b>	3,041.1 (13.1)	3,651.0 (90.7)	3,635.9 (38.7)	1,794.3 (776.4)	1,666.9 (269.6)	1,722.9 (408.2)
<b>l</b>	3,096.0 (3.5)	3,640.7 (79.6)	3,630.5 (50.0)	1,793.2 (707.3)	1,666.6 (189.3)	1,724.2 (391.9)
<b>m</b>	3,087.3 (6.9)	3,641.5 (84.3)	3,630.4 (50.0)	1,794.5 (721.1)	1,669.1 (205.1)	1,725.9 (394.5)
<b>n</b>	3,041.1 (13.1)	3,651.0 (90.7)	3,635.9 (38.9)	1,794.3 (776.4)	1,666.9 (269.6)	1,722.9 (408.2)
ADHPMs						
<b>a</b>	3,106.1 (3.4)	3,640.4 (73.8)	3,628.9 (45.2)	1,791.2 (718.2)	1,656.0 (337.5)	1,692.3 (151.4)
<b>b</b>	3,104.5 (3.6)	3,641.2 (74.4)	3,628.8 (42.5)	1,790.3 (731.1)	1,656.5 (337.6)	1,692.6 (149.3)
<b>c</b>	3,103.5 (3.9)	3,641.5 (75.5)	3,628.2 (42.5)	1,790.1 (740.1)	1,656.1 (342.2)	1,692.4 (148.8)
<b>d</b>	3,106.7 (3.2)	3,640.3 (72.3)	3,629.6 (45.3)	1,791.9 (703.2)	1,656.0 (282.8)	1,690.9 (152.2)
<b>e</b>	3,084.8 (6.0)	3,652.5 (71.9)	3,626.6 (35.5)	1,786.2 (730.7)	1,656.6 (389.1)	1,691.8 (156.4)
<b>f</b>	3,107.2 (7.7)	3,636.7 (74.1)	3,629.2 (48.1)	1,792.6 (712.5)	1,656.0 (349.3)	1,690.7 (146.0)
<b>g</b>	3,106.1 (2.9)	3,638.0 (74.0)	3,630.0 (48.6)	1,794.2 (696.9)	1,655.9 (336.1)	1,691.2 (146.2)
<b>h</b>	3,067.4 (9.0)	3,651.8 (83.5)	3,633.5 (40.9)	1,793.8 (771.9)	1,657.6 (385.3)	1,692.2 (135.9)
<b>i</b>	3,107.1 (4.5)	3,636.4 (73.5)	3,629.7 (48.8)	1,792.7 (711.0)	1,656.3 (350.1)	1,690.2 (144.6)
<b>j</b>	3,105.8 (3.1)	3,638.7 (73.7)	3,630.3 (47.9)	1,794.6 (688.9)	1,655.3 (336.1)	1,689.8 (138.9)
<b>k</b>	3,052.7 (7.1)	3,651.7 (83.7)	3,632.1 (40.2)	1,793.1 (761.5)	1,659.5 (380.3)	1,694.1 (130.3)
<b>l</b>	3,107.2 (3.0)	3,634.2 (73.2)	3,630.2 (55.4)	1,796.1 (705.8)	1,655.4 (268.7)	1,690.9 (143.8)
<b>m</b>	3,100.1 (4.2)	3,638.3 (80.2)	3,630.5 (47.6)	1,797.8 (722.7)	1,655.9 (377.3)	1,691.5 (138.8)
<b>n</b>	3,053.3 (4.0)	3,648.0 (89.3)	3,634.0 (38.1)	1,797.2 (791.9)	1,655.6 (435.8)	1,688.5 (132.1)

**Scheme 2**

in thermochemistry and kinetics of the oxidation reactions [34–36] of DHPMs are due only to the activation processes and the energetics of the transition states (TS) associated, of course, with the solvent effect. Thus, to be able to justify experimental kinetics data [34–36], it is necessary to work out the TS structures of the oxidation reaction, which is beyond the scope of the present work.

## Conclusions

The B3LYP/6-31++G(d,p) calculations show that the heterocyclic ring in all DHPMs has a flat *boat* conformation, and the aryl ring substituted at the C4 position prefers a *pseudo-axial* orientation. Furthermore, in the optimized structures of both ketonic and esteric DHPMs, the carbonyl group at the C5 position is oriented *s-trans* with respect to the C5=C6 bond of the DHPM ring, which is compatible with experimental data. The present calculations show that the charge density on the N3 atom is slightly higher than that on the N1 atom. Analysis of the deviations of the C4 and N1 atoms from the DHPM ring boat plane revealed the details of the intramolecular bonding and nonbonding interactions in these series of molecules. The deviation of the C4 atom from the boat plane is greater than that of the N1 atom. Calculated harmonic frequencies of the CO bond

**Table 6** Standard enthalpies of the formation and the oxidation reactions ( $\Delta H_f^\circ$ ,  $\Delta H_{ox}^\circ$ ) of some DHPMs calculated based on the B3LYP/6-31++G(d,p) optimized structures

The oxidation enthalpies are referenced to that of the corresponding **a** compounds

Comp.	$\Delta H_f^\circ$ (kJ/mol)		Reaction	$\Delta H_f^\circ$ (kJ/mol)		Reaction
	EDHPMs	EPMs		ADHPMs	APMs	
<b>a</b>	6,962.4	7,002.1	0.0	6,683.0	6,725.7	0.0
<b>b</b>	7,483.7	7,521.4	-1.4	7,203.5	7,245.2	-1.6
<b>c</b>	7,318.7	7,353.6	-3.6	7,038.8	7,077.5	-3.8
<b>d</b>	7,317.8	7,359.7	1.1	7,041.2	7,080.9	-2.8
<b>e</b>	7,319.9	7,375.1	10.9	7,044.1	7,375.1	-6.7
<b>f</b>	6,935.9	6,975.0	0.3	6,656.6	6,700.0	0.9
<b>g</b>	6,934.0	6,986.7	9.4	6,655.6	6,699.3	1.2
<b>h</b>	6,951.7	6,986.6	-3.8	6,672.2	6,708.1	-5.4
<b>i</b>	6,945.8	6,984.9	1.1	6,666.9	6,710.1	2.1
<b>j</b>	6,943.7	6,985.3	2.5	6,663.7	6,708.0	1.1
<b>k</b>	6,950.8	6,984.1	-5.3	6,669.7	6,709.4	-3.6
<b>l</b>	6,833.1	6,875.3	3.1	6,554.4	6,600.2	4.2
<b>m</b>	6,833.0	6,877.4	4.9	6,552.9	6,595.7	-0.3
<b>n</b>	6,867.8	6,887.8	-15.4	6,586.0	6,611.2	-15.1

stretching show the general order  $v_{C2=O9} > v_{C7=O8}$ , which is different from what was obtained in our experimental works, i.e.,  $v_{C7=O8} > v_{C2=O9}$ . This can be attributed to dimer formation under experimental condition, which is not taken into account in the single-molecule (gas-phase) calculations. To deduce any trend for the rate of oxidation reaction it is necessary to work out transition-state structures and energetics, which is underway in this research group.

## Computational methods

Structures of DHPMs were built and optimized preliminarily with semi-empirical PM3 method using HyperChem software [38]. These PM3 optimized structures were used as initial guess geometries for the ab initio calculations. Geometries of ethyl esters (EDHPMs) and the acetyl forms (ADHPMs) were optimized using the density functional theory (DFT) B3LYP method with 6-31++G(d,p) basis set. Structural and electronic characteristics calculated for the B3LYP/6-31++G(d,p) optimized geometries were analyzed in the following sections. All computations were carried out using the Gaussian98 package [39]. Compounds **1a** and **2a** (both with X = H) are considered as references to investigate comparatively the effect of the substitution on the aryl group at the C4 position on the optimized structures of EDHPMs and ADHPMs. Charge density distributions for all DHPMs were also studied using natural bond orbital (NBO) analysis of Weinhold [40–43].

**Acknowledgments** We are thankful to the Center of Excellence (Chemistry), Research Council, and Office of Graduate Studies of the University of Isfahan for financial support.

## References

- Nakamichi N, Kawashita Y, Hayashi M (2002) Org Lett 4:3955
- Kappe CO (1993) Tetrahedron 49:6937
- Kappe CO, Fabian WMF, Semones MA (1997) Tetrahedron 53:2803
- Kappe CO (2000) Eur J Med Chem 35:1043
- Atwal KS, Rovnyak GC, Kimball SD, Floyd DM, Moreland S, Swanson BN, Gougoutas JZ, Schwartz J, Smillie KM (1990) J Med Chem 33:2629
- Blacquiere JM, Sicora O, Vogles CM, Ćuperlović-Culf M, Decken A, Ouellette RJ, Westcott SA (2005) Can J Chem 83:2052
- Brands M, Endermann R, Gahlmann R, Krüger J, Raddatz S (2003) Bioorg Med Chem Lett 13:241
- Memarian HR, Sadeghi MM, Aliyan H (1998) Indian J Chem 37B:219
- Sadeghi MM, Memarian HR, Khosropour AR (1998) J Sci Islamic Repub Iran 9:240
- Memarian HR, Sadeghi MM, Momeni AR (1999) Indian J Chem 38B:800
- Memarian HR, Sadeghi MM, Momeni AR, Döpp D (2002) Monatsh Chem 133:661
- Memarian HR, Bagheri M, Döpp D (2004) Monatsh Chem 135:833
- Memarian HR, Abdoli-Senejani M, Döpp D (2006) Z Naturforsch 61B:50
- Memarian HR, Ghazaie M, Khakhki Mehneh S (2009) Z Naturforsch 64B:1187
- Shobha D, Adharvana Chari M, Ahn KH (2009) Chin Chem Lett 20:1059
- Kamaljit S, Sukhdeep S (2009) Tetrahedron 65:4106
- Ahmed B, Khan RA, Habibullah, Keshari M (2009) Tetrahedron Lett 50:2889
- Debach A, Amimour M, Belfaitah A, Rhouati S, Carboni B (2008) Tetrahedron Lett 49:6119
- Goldman S, Stoltzfuss J (1991) Angew Chem 103:1587
- Goldman S, Stoltzfuss J (1991) Angew Chem Int Ed 30:1559
- Memarian HR, Sabzyan H, Abdoli-Senejani M (2007) J Mol Struct (Theochem) 813:39
- Triggle DJ, Padmanabhan S (1995) Chemtract Org Chem 8:191

23. Rovnyak GC, Kimball SD, Beyer B, Cucinotta G, Dimarco JD, Gougoutas J, Berg AH, Malley M, Mc Carthy JP, Zhang R, Moreland S (1995) *J Med Chem* 38:119
24. Bikker JA, Weaver DF (1993) *J Mol Struct (Theochem)* 281:173
25. Palmer RB, Andersen NH (1996) *Tetrahedron* 52:9665
26. Langs DA, Kwon YW, Strong PD, Triggle DJ (1991) *J Comput Aided Mol Des* 5:95
27. Gaudio AC, Korolkovas A, Takahata Y (1994) *J Mol Struct (Theochem)* 303:255
28. Schnell B, Strauss UT, Verdino P, Faber K, Kappe CO (2000) *Tetrahedron Asymmetry* 11:1449
29. Kappe CO, Shishkin O, Uray G, Verdino P (2000) *Tetrahedron* 56:1859
30. Atwal KS, Swanson BN, Unger SE, Floyd DM, Moreland S, Hedberg A, ÓReilly BC (1991) *J Med Chem* 34:806
31. Krenn W, Verdino P, Uray G, Faber K, Kappe CO (1991) *Chirality* 11:659
32. Uray G, Verdino P, Belaj F, Kappe CO, Fabian WMF (2001) *J Org Chem* 66:6685
33. Fabian WMF, Semones MA, Kappe CO (1998) *J Mol Struct (Theochem)* 432:219
34. Memarian HR, Farhadi A (2009) *J Iran Chem Soc* 6:638
35. Memarian HR, Sabzyan H, Farhadi A (2009) *Z Naturforsch* 64B:532
36. Memarian HR, Farhadi A (2008) *Ultrason Sonochem* 15:1015
37. Kappe CO (1997) First international electronic conference on synthetic organic chemistry (ECSOC-1), September 1–30 (1997). <http://www.mdpi.org/ecsoc/posters/postersn.htm>. Accessed 25 Aug 2010
38. Hyperchem Release 7.0, Windows Molecular Modeling System, Hypercube, Inc. <http://www.hyper.com>. Accessed 25 Aug 2010
39. Frisch MJ, Trucks GW, Schlegel HB, Scuseria GE, Robb MA, Cheeseman JR, Zakrzewski VG, Montgomery JA, Stratmann RE, Burant JC, Dapprich S, Millam JM, Daniels AD, Kudin KN, Strain MC, Farkas O, Tomasi J, Barone V, Cossi M, Cammi R, Mennucci B, Pomelli C, Adamo C, Clifford S, Ochterski J, Petersson GA, Ayala PY, Cui Q, Morokuma K, Malick DK, Rabuck AD, Raghavachari K, Foresman JB, Cioslowski J, Ortiz JV, Stefanov BB, Liu G, Liashenko A, Piskorz P, Komaromi I, Gomperts R, Martin RL, Fox DJ, Keith T, Al-Laham MA, Peng CY, Nanayakkara A, Gonzalez C, Challacombe M, Gill PMW, Johnson B, Chen W, Wong MW, Andres JL, Head-Gordon M, Replogle ES, Pople JA (1998) Gaussian 98. Gaussian Inc, Pittsburg
40. Carpenter JE, Weinhold F (1988) *J Mol Struct (Theochem)* 169:41
41. Reed AE, Weinstock RB, Weinhold F (1985) *J Chem Phys* 83:735
42. Reed AE, Curtiss LA, Weinhold F (1988) *Chem Rev* 88:899
43. Xiao-Hong L, Zheng-Xin T, Xian-Zhou Z (2009) *J Mol Struct (Theochem)* 900:50